Vol. 55, No. 11

Interrogation of Related Clinical Pan-Azole-Resistant *Aspergillus fumigatus* Strains: G138C, Y431C, and G434C Single Nucleotide Polymorphisms in *cyp51A*, Upregulation of *cyp51A*, and Integration and Activation of Transposon *Atf1* in the *cyp51A* Promoter[▽][†]

Ahmed M. Albarrag,[1,2] Michael J. Anderson,[2] Susan J. Howard,[2] Geoff D. Robson,[3] Peter A. Warn,[2,4] Dominique Sanglard,[5] and David W. Denning[1,2,3,4]*

Department of Medical Microbiology, College of Medicine and University Hospital, King Saud University, Riyadh, Saudi Arabia[1]; School of Translational Medicine,[2] Faculty of Life Sciences,[3] and University Hospital of South Manchester,[4] The University of Manchester, Manchester Academic Health Science Centre, Manchester, United Kingdom and Institute of Microbiology, University of Lausanne, and University Hospital Center, Rue de Bugnon 48, CH-1011, Lausanne, Switzerland[5]

Multiple *Aspergillus fumigatus* isolates from a patient with two aspergillomas complicating chronic pulmonary aspergillosis were pan-azole resistant. Microsatellite typing was identical for all isolates despite major phenotypic and some growth rate differences. Three different *cyp51A* mutations were found (G138C, Y431C, and G434C), of which the first two were demonstrated by heterologous expression in a hypersusceptible *Saccharomyces cerevisiae* strain to be at least partly responsible for elevated MICs. *cyp51A* and *cyp51B* gene duplication was excluded, but increased expression of *cyp51A* was demonstrated in three isolates selected for additional study (7-to 13-fold increases). In the isolate with the greatest *cyp51A* expression, an *Aft1* transposon was found inserted 370 bp upstream of the start codon of the *cyp51A* gene, an integration location never previously demonstrated in *Aspergillus*. Two transcription start sites were identified at 49 and 136 bp upstream of the start codon. The role of the *Aft1* transposon, if any, in modulating *cyp51A* expression remains to be established. Increased mRNA expression of the transporters *AfuMDR1* and *AfuMDR4* also was demonstrated in some isolates, which could contribute to azole resistance or simply represent a stress response. The diversity of confirmed and possible azole resistance mechanisms demonstrated in a single series of isogenic isolates is remarkable, indicating the ability of *A. fumigatus* to adapt in the clinical setting.

Aspergillus fumigatus is a common saprophytic filamentous fungus with a worldwide distribution (33), and it is the most common etiological agent of aspergillosis. Invasive aspergillosis is associated with high morbidity and mortality (19), and in a recent case series chronic pulmonary aspergillosis was shown to have a 50% mortality rate during an 18-month period (26). It is estimated that there are over 3 million patients worldwide with allergic bronchopulmonary aspergillosis (8) and more than 1 million have chronic pulmonary aspergillosis (CPA) following tuberculosis (9). Azoles represent first-line therapy for all forms of aspergillosis and comprise the only class of drug available orally (44).

Azole resistance in *A. fumigatus* was first reported in 1997 when itraconazole-resistant isolates from two patients in the United States were described (10). Overall the reported frequency of azole resistance in *A. fumigatus* is approximately 2% (15), with great variation in different localities. The prevalence in The Netherlands is 6% (37). Likewise, in the Mycology Reference Centre Manchester culture collection, the frequency of azole resistance is now >8% (5, 16), predominantly

in CPA cases undergoing therapy. Both centers reported a continuing rise in azole resistance frequency.

Several mechanisms of azole resistance have been described for *Aspergillus* species. Triazoles are demethylase inhibitors and target the ergosterol biosynthetic pathway, an essential component of the fungal cell membrane, by binding to the Cyp51 family of cytochrome P450s, (sterol 14 α-demethylases), causing the depletion of ergosterol and the accumulation of lanosterol or eburicol and other toxic 14 α-methyl sterols (18). The most commonly reported azole resistance mechanism in clinical isolates of *A. fumigatus* is due to mutations in the target gene resulting in amino acid substitutions in sterol 14 α-demethylase that presumably reduce drug binding. There are two Cyp51 enzymes in *A. fumigatus* encoded by two genes, *cyp51A* (*pdmA*^{erg11}) and *cyp51B* (*pdmB*^{erg11}) (23). A number of missense mutations have been described in clinical isolates and in laboratory mutants, although almost all alterations linked with resistance are in *cyp51A* (15). Mutations in four codons (N22, G54, L98, and M220) have been shown to be the direct cause of resistance by replacing the wild-type copy of *cyp51A* in an *A. fumigatus* strain with a copy of the gene containing the putative resistance mutation (7, 11, 22, 25). Decreased intracellular azole accumulation has been demonstrated in one itraconazole-resistant clinical isolate and two laboratory mutants (10, 21), and several efflux pumps of the ABC transporter and major facilitator protein superclasses have been described in *A. fumigatus*, although none have been proven to date to play a

TABLE 1. MICs and *cyp51A* point mutations of eight pan-azole-resistant isolates from a CPA patient[a]

Isolate	Date of isolation (day/mo/yr)	MIC (mg/liter)					Amino acid substitution[b]
		AMB	ITR	VOR	RAV	POS	
F11628	23/01/2004	0.06	>8	>8	8	4	G138C
F12041	07/05/2004	0.25	>8	>8	>8	2–4	G138C
F12760	26/11/2004	0.125	>8	8	8	2	G138C
F12776	26/11/2004	0.125	>8	2–4	2–4	1–2	Y431C
F12865	07/12/2004	0.125	>8	8	8	2	G138C
F13535	29/04/2005	0.125	>8	8	8	2	G138C
F13746	17/06/2005	0.06	>8	8	8	2	G138C
F13747	17/06/2005	0.06	>8	4	4	1	G434C

[a] Data were determined from at least three separate experiments. AMB, amphotericin B; ITR, itraconazole; VOR, voriconazole; RAV, ravuconazole; POS, posaconazole.
[b] Sequence for all three codons of TGC.

direct role in resistance by pumping out azoles (6, 7, 27, 36, 40). Finally, an amino acid substitution at codon 98 (L98H) has been shown to cause pan-azole resistance, but it does so only when linked with a duplication of a 34-bp sequence in the 5′ upstream region of *cyp51A*, resulting in the upregulation of the gene (24). Neither mutation on its own was shown to be sufficient to cause resistance to azoles in transformants alone.

Having identified a sequential series of pan-azole-resistant isolates from a single patient, we investigated the mechanism of resistance in selected isolates and extended our investigation to determine the mechanistic causality of the mutations found, and we identified a transposon insertion upstream of *cyp51A*. These novel findings are highly significant in understanding azole resistance in *A. fumigatus*.

MATERIALS AND METHODS

Media. The following solid media containing 1.5% agar (Oxoid, Basingstoke, United Kingdom) were used: Sabouraud dextrose agar (SDA; Oxoid), 1% (wt/vol) glucose with Vogel's salts (VA [solid]) (43), and RPMI-1640 Auto-Mod buffered with morpholinepropanesulfonic acid (MOPS) to pH 7.0 and supplemented with 2% (wt/vol) glucose and 0.3 g/liter glutamine (RPMI; Sigma, Dorset, United Kingdom). In addition, the following broths were used: Sabouraud dextrose broth (SDB), 1% (wt/vol) glucose with Vogel's salts (VB [broth]), and RPMI-1640 Auto-Mod buffered and supplemented as described above. Sabouraud dextrose is a complex medium, Vogel's is a defined minimal medium, and RPMI is a defined medium routinely used for susceptibility testing.

Isolates. All eight isolates from a single patient were obtained from sputum samples (Table 1). Full case details have been published previously (17). In summary, the patient presented in 1999 with CPA with very large bilateral upper lobe aspergillomas. Itraconazole treatment was started in October 1999 at 200 mg/day, but despite treatment the patient's condition deteriorated. In January 2003, voriconazole treatment was started with slight improvement. In January 2004, his condition worsened again and intravenous caspofungin treatment was started at 50 mg six times weekly for more than 12 months. The patient died of respiratory failure in April 2006. All isolates are held in the Mycology Reference Centre Manchester culture collection. Two susceptible control isolates AF10 and AF41 (1) were used for real-time PCR, expression experiments, and transcription start site experiments. In addition, the sequence strain A1163 (12) was used as the control strain for heterologous transformation experiments, and the other sequence strain, AF293 (28), was used as an additional control for the *cyp51A* copy number determination. Control strains AF10, AF41 (both fully susceptible), and AF72 (azole resistant) were used in certain experiments.

Isolates of *A. fumigatus* were grown from −80°C glycerol (Sigma) stocks at 37°C for 7 days on SDA. Fresh spore suspensions were prepared in phosphate-buffered saline (PBS; Invitrogen, Paisley, United Kingdom) with 0.05% (vol/vol) Tween 80 (Sigma).

Antifungal susceptibility testing. Susceptibilities were determined on three separate occasions, using a modified European Committee on Antimicrobial

TABLE 2. List of novel primers used

Experiment and primer	Sequence (5′-3′)
PCR and sequencing of *cyp51B*	
cyp51B-F1	ACACTCAGCCTACCTTTATTCCCT
cyp51B-F2	CTCACTACGCCTGTTTTTGGTC
cyp51B-F3	CATGGTCTGGAACCTCATGTC
cyp51B-F4	GGTTAGTTAGCAAGGGCACCA
cyp51B-R1	ACACATAAATTTGGCAGCGA
cyp51B-R2	GGTTATGGTACAACTCTGCGAAT
cyp51B-R3	ATATGAAGTACCATCCACAGCCA
cyp51B-R4	TTCCATGCAAGTCTATCAAGAAGAG
PCR and sequencing of 5′ upstream region of *cyp51A*	
cyp51Apro-1[a]	GTGACAAGCGAAGATTCCACACAT
cyp51Apro-2	ACAACAGAAGCGACTTTCTCTTCAG
cyp51Apro-3	GTCTTTAGATTCGGTGGACGC
cyp51Apro-4	GCTGCCGCTGAGGAACATATG
cyp51Apro-5[a,b]	GTAAGCCATAGCATCGGCACCAT
F12776PR5walk1	GCCTAGAATATGGCAGTCACTGC
F12776PR3walk1	TTATACTACCCTCCAGCGGC
Gene copy no. determination (*cyp51A*)	
cyp51AgDNAq1	AGAGGTCTATAGTCCATTGACGA
cyp51AgDNAq2[b]	TCCTTCTCAATAAGTGGCACA
benA-gDNA-1	ATTCAGGAGTTGTTCAAGCG
benA-gDNA-2	GTACTGCTGGTATTCGGAGAC
Gene expression	
cyp51AqPCRfor	TGCAGAGAAAAGTATGGCGA
cyp51AqPCRrev	CGCATTGACATCCTTGAGC
cyp51BqPCRfor	AGCAGAAGAAGTTCGTCAAATAC
cyp51BqPCRrev	TCGAAGACGCCCTTGTG
MDR1for	TTCCCTTGTTCACAATTCTCTTCG
MDR1rev	TGACATAGACTGTGACAAACTCG
MDR2for	TTTAGCTCCACCGGGTTTG
MDR2rev	TCGAAAGACCGAACATGCTTGA
MDR3for	TCTGATGGCGGTCATCACT
MDR3rev	ATATCCATCCCCCAGGC
MDR4for	TATGGCTTAGTTTGTGTCACCGA
MDR4rev	AGAGCAATTCGTTGCTTCTG
atrF-for	AGAGAAATCGGACAACTGCTGA
atrF-rev	CCTCGTCGCAGATAGTCTTGTA
benA-for	CTGTATCGACAACGAGGCTCT
benA-rev	AGTTGAGCTGACCAGGGAAA

[a] Primer used for both PCR and sequencing.
[b] Primer used for 5′ RACE.

Susceptibility Testing (EUCAST) method (39) with a lower final inoculum concentration of 0.5×10^5 CFU/ml (16). Isolates were tested at a final drug concentration range of 8 to 0.015 mg/liter against itraconazole (Research Diagnostics, Concord, CT), voriconazole (Pfizer, Sandwich, United Kingdom), ravuconazole (Bristol Myers Squibb, New York, NY), posaconazole (Schering-Plough, NJ), and amphotericin B (Sigma). Clinical breakpoints have not been established for *Aspergillus* species and azoles; however, epidemiological cutoffs have been proposed for itraconazole, posaconazole, and voriconazole (32, 34, 42). Following these proposals, the following cutoffs were used during this study: itraconazole and voriconazole, >2 mg/liter; posaconazole, >0.5 mg/liter.

DNA extraction, PCR, sequencing, and Southern hybridization. DNA extractions and purifications were performed as described previously (1). Microsatellite typing was carried out as described by Bart-Delabesse et al. (4). Primers for the amplifying and sequencing of *cyp51A* and *cyp51B* and the 5′ upstream region of *cyp51A* are listed in Table 2, and conditions were as previously described (17). Restriction endonuclease digestions, agarose gel electrophoresis, and alkali transfer of DNA onto positively charged nylon membranes were performed using standard methodologies. The digoxigenin (DIG) labeling and chemilumines-

cence detection system (Roche) was used with one PCR-derived *Aft1* probe amplified from F12776 genomic DNA, using primers shown in Table 2, with the same conditions as those for *cyp51A* and *cyp51B* amplification.

Expression and gene copy number analysis using real-time PCR. Nephlos shake flasks containing 40 ml of VB (defined medium) and inoculated with 1×10^7 spores per ml (final) were incubated at 35°C until the cultures reached an optical density at 580 nm (OD_{580}) of 6.0 to 6.5, at around 16 h of growth. For expression in the presence of itraconazole, cultures were grown to an OD_{580} of 3.0 to 3.5 (mid-logarithmic phase grow) before adding 4 mg/liter of itraconazole in 20% (wt/vol) cyclodextrin. Control flasks with cyclodextrin only also were analyzed. Two-milliliter samples were removed at 0, 1, 2, and 4 h. Cultures were repeated on another day so that four flasks in total were grown for each isolate. Two RNA extractions were carried out from each culture from 50 to 100 mg (wet wt) of mycelium, snap-frozen in liquid nitrogen, using a Qiagen RNeasy Plant Minikit (Qiagen, West Sussex, United Kingdom). RNase-free DNase I (Qiagen) was used to ensure the complete removal of all genomic DNA. RNA concentrations and purity were determined using a NanoDrop ND-1000 spectrophotometer. Primers used for real-time PCR are listed in Table 2. Finally, all reverse transcription-PCRs (RT-PCRs) were designed so that one of the primers spanned an exon-exon junction in the target cDNA. Primer specificities were confirmed by the presence of single bands only on agarose gels and by sequencing PCR products. Dissociation curve analyses were performed after all real-time PCRs to confirm the presence of single peaks only over the entire temperature range. Real-time PCR was carried out with the Mx3000P Real-Time PCR system (Stratagene) with Brilliant SYBR green QPCR master mix or a Brilliant SYBR green QRT-PCR master mix one-step kit (Stratagene). Each RNA and DNA sample was analyzed twice. Twenty-microliter reaction mixtures were set up with 100 nM each primer and 25 ng of genomic DNA or 150 ng of RNA, distributed into 96-well PCR plates (ABgene), and sealed. Three controls were included: no-primer, no-template, and no-reverse-transcriptase controls. The amplification program for RNA was 50°C for 1 h for reverse transcription, followed by one cycle of 10 min at 95°C and then 40 cycles of 95°C for 30 s, 60°C for 60 s, and 72°C for 60 s, whereas for DNA the RT step was omitted.

Determination of the transcription initiation site of *cyp51A*. The transcription initiation site was determined by using rapid amplification of cDNA ends (RACE) using the 5′ RACE system, version 2.0 (Invitrogen). Primer Afcyp51A709R (Table 2) was used for first-strand cDNA synthesis with the primers CYP51A-gDNA-q2 and CYP51A-pro-5, which were used in combination with a deoxyinosine-containing anchor primer for the two subsequent PCRs. First-strand cDNA synthesis was carried out with 2 μg of total RNA and SuperScript II reverse transcriptase in duplicate. Controls included using dTTP instead of dCTP for tailing and no reverse transcriptase. PCR products were analyzed on 3% NuSieve 3:1 agarose gels (FMC BioProducts). DNA was extracted from gels using the QIAquick gel extraction kit (Qiagen) and sequenced.

Growth rate measurements. Colony radial growth rate measurements were performed on SDA, VA, and RPMI. For each isolate, 2.5 μl of 1×10^6 CFU/ml was inoculated into 25 ml medium. Plates were incubated at 35°C for 4 to 5 days, and colony diameters were measured twice daily using a Shadow Master (Beaty and Co., United Kingdom) at 10× magnification (35).

The specific growth rate was measured using a spectrophotometric microbroth method (30). Spore suspensions were diluted 1:5 in SDB, VA, and RPMI to give a final concentration of 2×10^5 CFU/ml; 50 μl was pipetted in quadruplicate into 96-well microtiter plates incubated with shaking at 37°C, and ODs were measured every 5 min for 24 h. It was not possible to determine specific growth rates in RPMI or VA, as uniform and conventionally shaped growth curves were not obtained.

Determination of hyphal growth unit length. The hyphal growth unit length was determined on SDA, VA, and RPMI. Agar was inoculated with 100 μl of 3×10^2 CFU/ml spores and then overlaid with sterile cellophane membrane (BT14; British Cellophane, Twickenham, United Kingdom). The plates were incubated at 35°C for 16 h, after which images of germlings with seven or more tips were taken (analyzed using ImageJ software from the NIH), and hyphal growth unit length calculated by dividing total germling length by the number of tips (35).

Determination of conidial yield. Conidial production was assessed as described previously, with some modifications (3). One hundred μl of a 1×10^6 CFU/ml suspension was spread onto SDA, VA, and RPMI in duplicate and incubated at 35°C for 5 days. Four agar plugs were removed from each plate using a sterile 6-mm-diameter stainless-steel cork borer. Each plug was homogenized in 2 ml phosphate-buffered saline (PBS) with 0.05% (vol/vol) Tween 80, two counts were performed using a hemocytometer, and the means were calculated.

Determination of percentage of germination. The determination of the percentage of germination was performed as described previously (2) and was measured in SDB, VB, and RPMI. A final concentration of 5×10^5 CFU/ml in

15 ml of medium was incubated at 35°C with shaking. Aliquots (0.1 ml) were removed at hourly intervals, and the proportion of spores that had germinated was determined. Spores were considered to have germinated when the length of the germ tube was at least half the diameter of the conidium. A total of 200 spores were counted for each determination. Experiments were carried out in duplicate.

Functional complementation of *erg11* in *Saccharomyces cerevisiae*. Information on the functional complementation of *erg11* in *Saccharomyces cerevisiae* is provided in the supplemental material.

Quantitative and statistical analyses. (i) Real-time PCR. Eight and replicate samples were analyzed for the expression studies and the gene copy number study, respectively. Each expression experiment was repeated once with fresh spores, with two RNA extractions performed per culture and two PCRs carried out per RNA sample. The *benA* gene encoding β-tubulin, as described by Pfaffl et al. (17), was used for normalizing both gene copy number and transcript levels, and final results were given relative to the appropriate reference gene and AF10. This method combines the normalization and amplification efficiencies of the target gene with the calibrator, an untreated control, and is represented as the expression at time zero. The *benA* gene is known to be a single-copy gene, and it has been found to be expressed constitutively and is not affected by experimental conditions, such as itraconazole treatment (Paul Bowyer, personal communication). For all PCRs, the square regression correlation coefficients (R^2) ranged between 0.989 and 1.000. PCR amplification efficiency was calculated using the following formula: efficiency (E) = $10^{(1/slope)}$. The efficiency of each replicate varied from 1.9 to 2.1, which was acceptable. The optimal threshold was chosen automatically and was used to calculate the threshold cycle (C_T) for samples. Relative values of the target genes were normalized to the control gene, *benA*, as described by Pfaffl et al. (31), and final results are given relative to the appropriate reference gene and AF10. This method combines the normalization and amplification efficiencies of the target and reference genes to correct for differences between the two assays using the relative expression software tool (REST). For the calibrators, the change in C_T is set to equal 0, and therefore the fold change in gene expression for the control is equal to 1. In the time course study, the calibrator, an untreated control, represented expression at time zero.

(ii) Fitness. All calculations were performed using SPSS v13.0. All experiments were carried out at least twice on different days with at least quadruplicate measurements taken for each time point. Statistical analyses involving two groups were made by Student's *t* test, whereas analysis of variance (ANOVA) multiple-comparison tests were used to compare more than two groups. For growth rates, each replicate was analyzed separately before the rates were combined to give the means ± standard errors of the means (SEM). The linear portions of the growth curves were used for statistical analysis. The colony radial growth rate was calculated as described previously (35). The specific growth rate was analyzed as described previously (30). For the conidiation and germination experiments, the replicates from both experiments were expressed as the means before the two means were combined to give the overall value ± SEM. Hyphal growth unit length, in μm, was calculated as the ratio between the total length of the mycelium and the number of hyphal tips (41).

RESULTS

The susceptibilities of the tested isolates are shown in Table 1. Applying the proposed interpretative breakpoints (32, 34, 42), all eight isolates were considered to be pan-azole resistant. The isolates were susceptible to amphotericin B and caspofungin (data not shown) (17).

Phenotypic characterization of the isolates. Six of the isolates produced typical colony morphologies for *A. fumigatus*, where rapid conidiation results in gray-green colonies (Fig. 1). In contrast, isolate F12776 produced smaller colonies (Fig. 1), and F13747 produced poorly sporulating colonies. Growth rate, conidial yield, and percent germination data are summarized in Table 3. The quantitative experiments confirmed our initial observations, where F12776 had a reduced colony radial growth rate relative to those of the other isolates (e.g., on RPMI, 50 versus 349 μmh^{-1}; $P < 0.01$), and F13747 and F12776 produced fewer spores per mm^2 (e.g., on RPMI, 0.4×10^6 and 0.6×10^6 versus 8×10^6 to 10×10^6 for the other
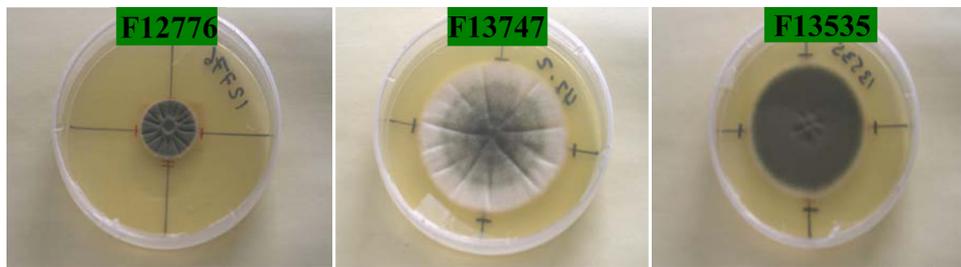
FIG. 1. Colony morphology of three of the isolates on SDA medium after incubation at 35°C for 96 h. The colony diameter of F12776 was 30 to 35 mm and was 60 to 70 mm for the other two isolates. F13535 is an example of the morphology of the majority of the isolates.

strains). Interestingly, F12776 had a significantly faster specific growth rate than all of the other isolates, whereas F13747 had a significantly slower one (0.160 for F12776, 0.142 for F12760, and 0.119 for F13747 in SDB; $P < 0.01$). Finally, it was noted that F13747 germinated more slowly than the other isolates (Fig. 2); in SDB, 32% of F13747's conidia had germinated at 8 h, whereas an average of 74% of conidia had germinated for the other seven isolates.

The majority of the isolates had a typical microscopic morphology for *A. fumigatus*. The germlings of F12776, on the other hand, were more compact and swollen, and the hyphae showed increased branching. A quantitative determination of branching confirmed this observation.

Molecular characterization of the isolates. Molecular typing showed that all eight isolates were the same type [A, $(CA)_9(GA)_{10}$; B, $(CA)_2C(GA)_{10}$; C, $(CA)_{13}$; and D, $(CA)_{18}$] (17). The G138C substitution identified in the *cyp51A* gene was found in all isolates except F12776 and F13747 (Table 1). Two novel amino acid substitutions were found: Y431C in F12776 and G434C in F13747. Two silent mutations in codons S216S (C648T) and P394P (T1182G) were identified in the *cyp51B* gene of all eight isolates (data not shown). Real-time PCR was carried out to calculate gene copy numbers and demonstrated that single copies of *cyp51A* were present in F12760, F12776, and F13747. The reference strain used was AF293. Hence, no target gene amplification had occurred as a mechanism for resistance.

Real-time reverse transcriptase PCR was carried out on *cyp51A*, *cyp51B*, and five genes that have been postulated to have a role in azole resistance. Gene expression was studied in

three isolates (F12760, F12776, and F13747) during mid-logarithmic growth in defined minimal medium, and values were normalized to those for *benA*. Statistically significant differences were observed in the expression of *cyp51A*, *AfuMDR2*, and *AfuMDR4* genes (Fig. 3). F12776 had a higher level of *cyp51A* expression (2.9×) than AF41, as did the other two isolates (2.1× for F12760 and 1.6× for F13747), whereas *AfuMDR2* and *AfuMRD4* had similar expression profiles, with the highest expression in F12760 followed by that in F12776 and then F13747. It is particularly noteworthy that the expression of the *cyp51A* gene in all three isolates was considerably higher than that in other isolates that we have studied, including three unrelated azole-susceptible isolates and the isogenic azole-resistant pair of two of these (9.6-, 13.4-, and 7.2-fold higher expression for F12760, F12776, and F13747, respectively, than the expression of susceptible isolate AF41). The effect of itraconazole on gene expression also was studied during a 4-h time course. A concentration of itraconazole was used that had no effect on the growth of these three pan-azole-resistant isolates but that had been shown to reduce the growth of an azole-susceptible isolate by 50%. Values were expressed relative to that of a cyclodextrin control (used to eliminate any potential impact on expression from cyclodextrin, which is used to solubilize itraconazole clinically), and only those genes where a statistically significant increase in expression during the time course was observed are shown in Fig. 4. The expression of *cyp51A* and *cyp51B* increased only in F13747, and the largest increase was only 2-fold for *cyp51A* at 4 h. Far larger increases were observed in an azole-susceptible isolate (AF41), as might be expected when ergosterol production has been

TABLE 3. Determinations of growth rates, conidial yields, and percent germination at 8 h[a]

Isolate	Colony radial growth rate[b] in (μm · h^{-1}):			SDB specific growth rate (h^{-1})[b]	Conidial yield[c] in (1×10^6 conidia/mm^2):			% Germination at 8 h[d] in:		
	SDA	RPMI	1% GLU		SDA	RPMI	1% GLU	SDB	RPMI	1% GLU
F11628	431	372	334	0.142	64.2	9.1	24.3	75	70	31
F12041	425	352	324	0.142	65.2	10.6	23.6	71	71	32
F12760	395	338	289	0.147	78.1	8.2	23.7	73	70	30
F12776	127*	50*	127*	0.160*	21.5*	0.6*	4.7*	78	72	33
F12865	418	348	319	0.138	72.0	8.2	18.9	74	70	32
F13535	384	360	292	0.142	51.6	10.7	19.4	74	71	33
F13746	407	331	288	0.144	51.7	8.4	18.2	72	69	31
F13747	411	343	294	0.119*	7.0*	0.4*	3.3*	32*	32*	10*

[a] All experiments were repeated once. *, $P < 0.01$.
[b] The growth rates of each replicate (8 or 16) were calculated before being averaged.
[c] Averages from 16 replicates.
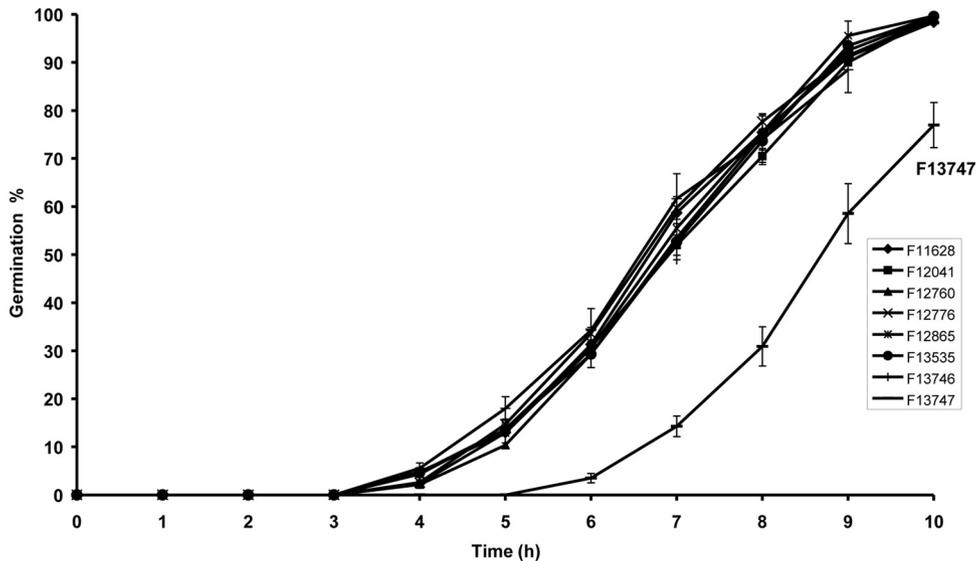[d] Averages from 8 replicates.

FIG. 2. Germination of conidia from all eight isolates. Counts were measured at hourly intervals in SDB at 35°C. Each point represents the means from eight replicates ± standard deviations. Typical apical hyphae grow singly or with a bifurcate structure, lateral branches that tend to grow out perpendicularly, and hyphae that grow relatively straight. F122776, however, showed atypical swollen hyphae that did not grow in straight lines.

restricted and a positive feedback mechanism is activated (up to 7.5-fold relative to the level for the untreated control at 4 h for *cyp51* [data not shown]). Increasing amounts of mRNA were seen for *AfuMDR1* in F12760, for *AfuMDR3* in F12776, and for *AfuMDR4* in F12776 and F13747, although the increases generally were significantly different only at 4 h and were less than 2-fold higher than those in controls.

As the expression level of *cyp51A* in the three isolates studied was considerably higher than in those of other isolates that we have measured, the region upstream of the start codon was sequenced as a starting point for a molecular explanation. No nucleotide substitutions were identified in 1,719 bp upstream of the ATG start in F12760 and F13747 compared to the sequence of two azole-susceptible isolates. In contrast, a 1,822-bp insertion was found in F12776 370 bp upstream of the start codon in the same orientation as *cyp51A*. The insertion has all the features of a type II transposon with a 100% conserved 45-bp terminal inverted repeat and a single open reading frame (ORF) encoding a transposase of 556 amino acids. The transcriptional start sites (TSS) were determined using 5′
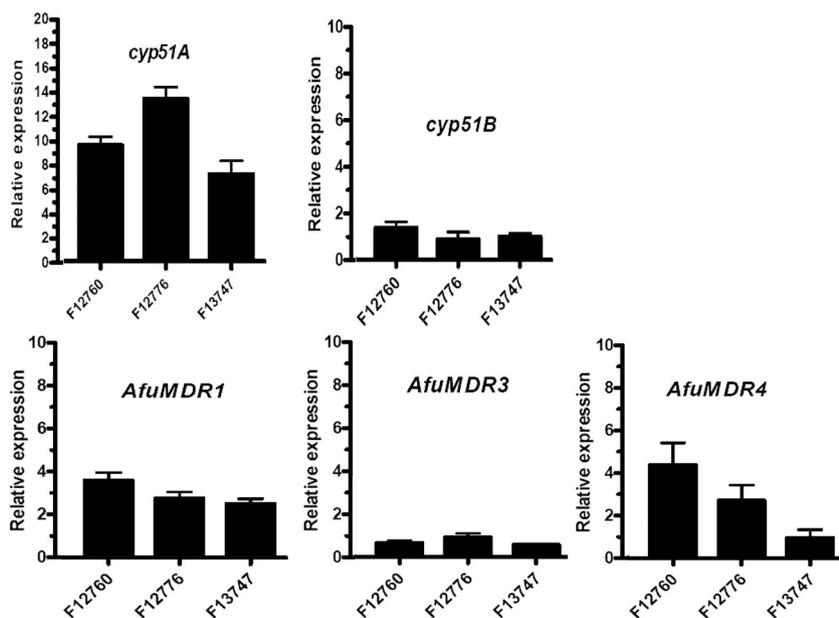

FIG. 3. Relative expression levels of the five *cyp51A*, *cyp51B*, *AfuMDR1*, *AfuMDR3*, and *AfuMDR4* genes in three of the isolates. Expression was normalized to β-tubulin and is the means from four experiments.
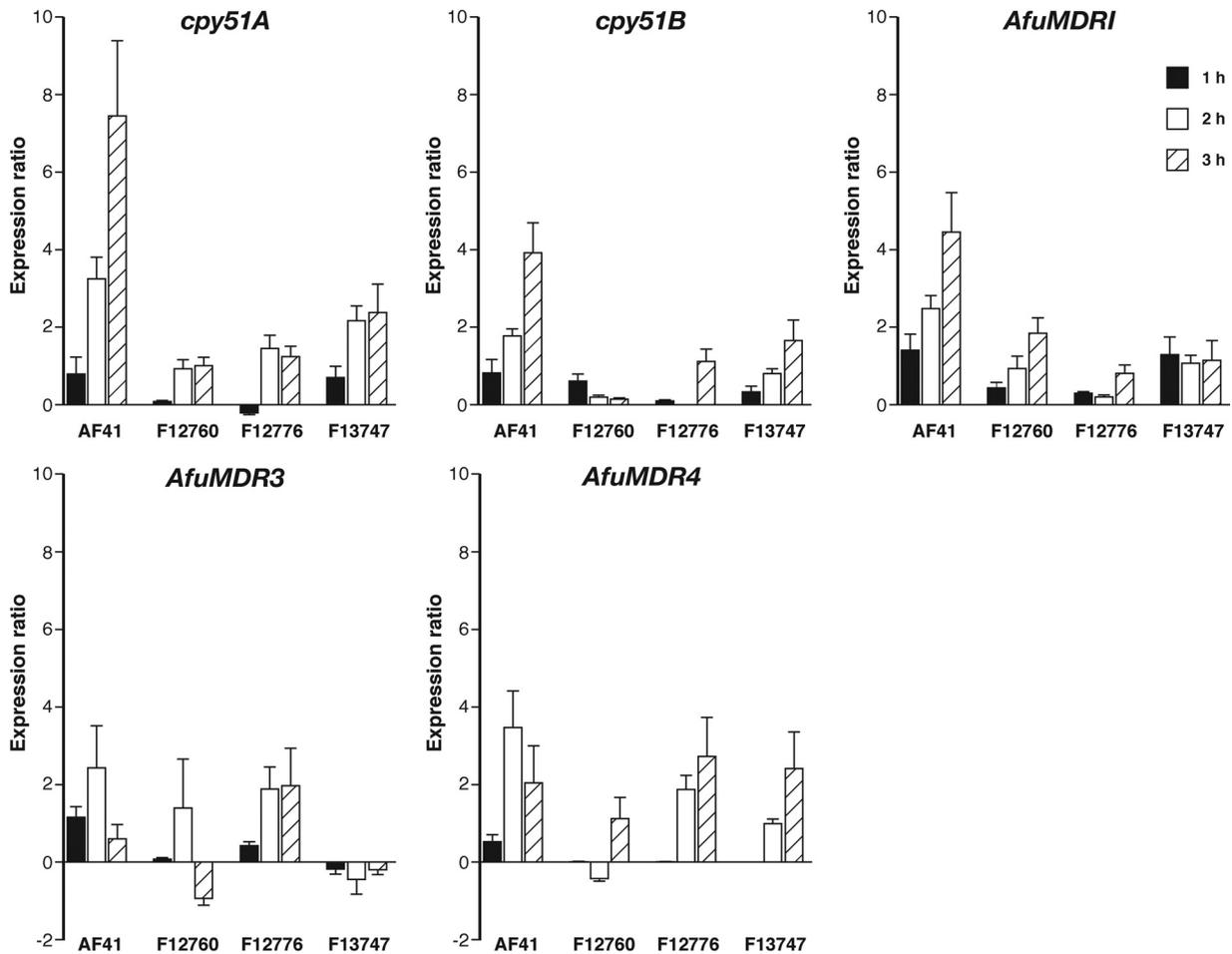
FIG. 4. Effect of itraconazole treatment on the expression levels of five genes in three of the isolates and the susceptible isolate AF41. Expression was determined at 1, 2, and 4 h after the addition of 4 mg/liter ITR and is compared to that at 0 h. Values are expressed relative to those for a cyclodextrin control. The results represent the results from two independent experiments performed in duplicate. Significant differences are indicated by asterisks ($P < 0.05$).

RACE for F12760 and F12776, as well as for two unrelated azole-susceptible clinical isolates (AF41 and AF10) and the azole-resistant isogenic pair of one of them (AF72). Two TSSs were identified lying 49 and 136 bp upstream of the start codon. As judged by the intensity of the amplified RACE products on agarose gels, F12760 and F12776 utilized only the −136 TSS, whereas the other three isolates utilized both TSSs to a similar extent (data not shown). Based on this evidence, the insertion of a transposon 234 bp upstream of the TSS did not have any effect on the initiation site for transcription.

Since both the sequencing data and the multilocus microsatellite typing indicate that *Aft1* had transposed into the promoter of *cyp51A* while this strain was growing in the patient, Southern hybridizations were carried out using four restriction nucleases to identify the overall distribution of this transposon in five out of the eight isolates. The earliest available isolate (F11628), as well as the two obtained at the same time as F12776 (F12760) and F13747 (F13746), were analyzed with restriction enzymes where the expected size of the *cyp51A* fragment was of a reasonable size to resolve on an agarose gel. The Southern hybridizations using internal *Aft1* probes of EcoRI and BglI digestions are shown in Fig. 5. Similar results

were obtained with BamHI and KpnI (data not shown). Twenty hybridizing bands were distinguishable on three of the gels in four of the isolates with identical banding patterns being observed. Only 19 bands could be resolved on the KpnI gel where, in general, fragment sizes were larger. In contrast, differences in the pattern of hybridizing bands were observed in F12776 compared to those of the other four isolates. The same 19 or 20 bands were observed in the KpnI, BamHI, and BglI digestions, whereas 1 band of approximately 12 kb was missing and another of ~7.5 kb was present (Fig. 5). More noteworthy, however, was the observation of a unique band only present in F12776 for each of the four digestions. These four bands were of the expected sizes to represent the copy of *Aft1* upstream of the *cyp51A* gene.

Functional complementation in *S. cerevisiae* of *cyp51A* alleles associated with azole resistance. The three *cyp51A* mutations associated with pan-azole resistance in the isolates from the CPA patient were transformed into *S. cerevisiae* to address their involvement in azole resistance. Alleles of *cyp51A* with the G138C, Y431C, or G434C mutations were amplified from total cDNA, cloned into a yeast shuttle vector (YEp51), and transformed into an *S. cerevisiae* mutant lacking the en-
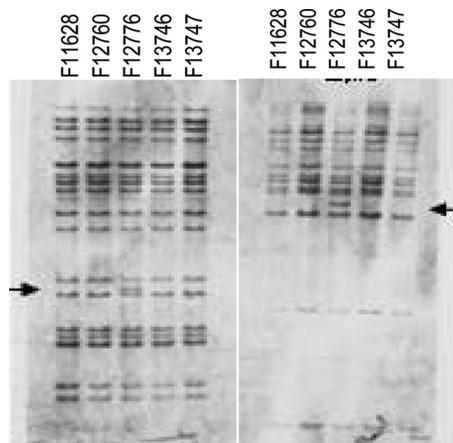
FIG. 5. Southern hybridizations of restriction digestions of genomic DNA from five of the isolates. (A) A BglI digestion hybridized with a 282-bp *Aft1* probe derived from PCR carried out on F12776 DNA. A band (indicated by the arrow) of approximately 4.9 kb is present only in the F12776 lane; the expected size is 4,892 bp. (B) An EcoRI digestion hybridized with a 282-bp *Aft1* probe derived from a PCR carried out on F12776 DNA. A band (indicated by the arrow) of approximately 7.5 kb is present only in the F12776 lane; the expected size is 7,522 bp. In addition, a band (indicated by an oval) of approximately 12 kb is missing from the F12776 lane, and two bands (indicated by asterisks) have not hybridized with the same intensity as in the other four lanes. The positions of the size markers are indicated on the left side of the gels. Hyperladder I (Bioline) and λ DNA monocut mix (New England BioLabs) were used.

dogenous *ERG11*, the target gene for azoles, and *PDR5*, a gene encoding an efflux pump known to include azoles among its substrates.

The susceptibilities of *S. cerevisiae* transformants containing individual *cyp51A* cDNAs were tested by spotting 10-fold serial dilutions containing various concentrations of itraconazole, voriconazole, and posaconazole (see Fig. S1 in the supplemental material). These mutants were compared to a haploid mutant containing a *cyp51A* allele from a susceptible strain of *A. fumigatus*. The transformants carrying the G138C and Y431C mutations were approximately 10-fold less susceptible to all three azoles than the control transformant (see Fig. S1). In contrast, and unexpectedly, the G434C mutant was hypersusceptible, with no growth occurring at any dilution of cells and for all drug concentrations (see Fig. S1). Similar results were obtained for the other three duplicate mutants (data not shown). Immunodetection by Western blotting with anti-*A. fumigatus* Cyp51A antibody carried out on the same cultures as those used for the susceptibility assay confirmed that similar amounts of protein had been expressed during this experiment for all six transformants (data not shown). In addition, the G138C form of the protein had a slightly reduced mobility relative to that of the other Cyp51A proteins.

DISCUSSION

All eight isolates from a single patient case were pan-azole cross-resistant. Two isolates (F12776 and F13747) had different mutations in the *cyp51A* gene (Y431C and G434C) from the rest (G138C). Alteration G138C has been identified previously in an azole-resistant laboratory mutant (20). However, substitutions Y431C and G434C have not been reported in

clinical isolates or laboratory mutants to our knowledge (16). The heterologous expression of *cyp51A* in *S. cerevisiae* confirmed that two of the missense mutations (G138C and Y431C) were at least partly responsible for azole resistance. The heterologous expression of the G434C *cyp51A*, however, resulted in an unexpected hypersusceptible phenotype, raising questions about the impact of this substitution on *cyp51A* and why this strain was azole resistant. Our supposition is that heterologous expression in yeast is not a perfect model for single nucleotide polymorphisms at the carboxy end of the protein. Perhaps there is second-order confounding of protein-protein interactions not existing in *Aspergillus* and the possible loss of the anchoring of the protein. Additional work using an *Aspergillus*-based heterologous system is probably required to dissect out how G434C confers azole resistance, because our other mechanistic studies do not fully explain this.

In addition to the *cyp51A* sequence, these isolates showed further divergence despite having the same microsatellite type. Phenotypically F12776 (Y431C) was significantly slower growing, and both it and F13747 (G434C) sporulated poorly. In filamentous fungi, hyphal extension and branching frequency are interdependent, and the following relationship has been established: $E = G\mu$, where E is the mean rate of hyphal extension, G is the hyphal growth unit length (mean hyphal length per hyphal tip in a mycelium), and μ is the specific growth rate (38). The hyphal growth unit length for F12776 was significantly smaller (163 μm for F12776, 243 μm for F12760, and 259 μm for F13747 on SDA; $P < 0.01$). So even though F12776 has a higher specific growth rate than all other isolates, its mean rate of hyphal extension is less than those of the other isolates (26 for F12776, 31 for F13747 and 36 for F12760) and would be expected to produce smaller, more compact colonies.

Previously the primary mechanism of resistance reported in azole-resistant *A. fumigatus* has been alterations to the target gene *cyp51A*. However, there is mounting evidence of the contribution of other mechanisms (5). In addition to mutations in *cyp51A*, the expression of this gene was found to be higher in these isolates than in others tested. The increased expression of the homologous gene in *cyp51A* in *Candida* (*erg11*) has been linked with resistance (13). In *A. fumigatus*, the duplication of *cyp51A* resulted in a rise in MIC (29) and a tandem repeat in the promoter region of the *cyp51A* gene that leads to upregulation (accompanied with mutations at codon 98) also conferred resistance (24). The increase in *cyp51A* expression in the case described here may be the result of the translocation and activation of a single copy of a multicopy transposon into the 5′ upstream region of *cyp51A*, probably into the promoter region. This *A. fumigatus* transposon has been characterized in a previous study, where it was clustered with other fungal elements of the *Fot1/Pogo* group and labeled *Aft1* (14). Hey et al. (14) demonstrated that all 10 clinical isolates studied had copies of this transposon variably distributed around their genomes, although one of them contained a truncated form of ~1.7 kb. They further showed that its target site is TA, which is duplicated after insertion. This duplication was found in the upstream region of F12776.

Of potential importance in the induction of resistance is the finding that a susceptible isolate, AF41, had a remarkable increase in *cyp51A* expression with itraconazole, unlike the

other susceptible isolate, AF10. AF41 is the same molecular type as AF72, which was one of the first two resistant isolates reported, and it was isolated from the same patient (10). AF72 has a *cyp51A* G54 mutation. If some isolates are able to survive azole therapy by upregulating *cyp51A*, it may be that subsequent mutations could emerge. The upstream tandem repeat associated with L98H could contribute to the emergence of resistance using this mechanism.

The molecular typing of the isolates confirmed that they all were identical. Because of the high discriminatory power of this typing technique, the most parsimonious explanation for the isolates having the same type is that the patient was originally infected by a single strain, which developed resistance and further evolved *in situ* within the lung. Azole resistance must have evolved independently more than once within this patient, as *cyp51A* mutations were not accumulated. We have additional evidence of *in situ* evolution from other patients who have developed azole resistance in aspergillomas but through different mechanisms (16).

In conclusion, this study on isolates obtained during 2 years from a single patient with bilateral aspergillomas has generated a number of unique findings. Most notable are a novel SNP (Y431C) conferring high-level azole cross-resistance and confirmation that another SNP (G138C) we previously reported is the cause of azole resistance. Also novel for *Aspergillus* is the concomitant and variable upregulation of *cyp51A* and the variable inducibility of *cyp51A* in different strains with itraconazole. Some alteration in transporter expression is intriguing. For the first time in clinical isolates we have observed the movement of a transposon, and this caused us to identify two upstream transcription sites of *cyp51A* for the first time. The transposon insertion also might be responsible for the increased expression of *cyp51A* in the azole-resistant isolates.

REFERENCES

1. **Anderson, M. J., K. Gull, and D. W. Denning.** 1996. Molecular typing by random amplification of polymorphic DNA and M13 Southern hybridization of related paired isolates of *Aspergillus fumigatus*. J. Clin. Microbiol. **34:**87–93.
2. **Araujo, R., and A. Rodrigues.** 2004. Variability of germinative potential among pathogenic species of *Aspergillus*. J. Clin. Microbiol. **42:**4335–4337.
3. **Balajee, S. A., J. L. Gribskov, H. Edward, D. Nickle, and K. A. Marr.** 2005. *Aspergillus lentulus* sp. nov., a new sibling species of *A. fumigates*. Eukaryot. Cell **4:**625–632.
4. **Bart-Delabesse, E., J. F. Humbert, E. Delabesse, and S. Bretagne.** 1998. Microsatellite markers for typing *Aspergillus fumigatus* isolates. J. Clin. Microbiol. **36:**2413–2418.
5. **Bueid, A., et al.** 2010. Azole antifungal resistance in Aspergillus fumigatus: 2008 and 2009. J. Antimicrob. Chemother. **65:**2116–2118.
6. **Chen, J., H. Li, R. Li, D. Bu, and Z. Wan.** 2005. Mutations in the *cyp51A* gene and susceptibility to itraconazole in *Aspergillus fumigatus* serially isolated from a patient with lung aspergilloma. J. Antimicrob. Chemother. **55:**31–37.
7. **Da Silva Ferreira, M. E., et al.** 2004. In vitro evolution of itraconazole resistance in *Aspergillus fumigatus* involves multiple mechanisms of resistance. Antimicrob. Agents Chemother. **48:**4405–4413.
8. **Denning, D. W., A. Pleuvry, and D. C. Cole.** 2010. Global burden of allergic bronchopulmonary aspergillosis (ABPA) complicating asthma. Thorax **65**(Suppl. 4):A155–A155.
9. **Denning, D. W., A. Pleuvry, and D. C. Cole.** 2010. Global burden of chronic

10. **Denning, D. W., et al.** 1997. Itraconazole resistance in *Aspergillus fumigatus*. Antimicrob. Agents Chemother. **41:**1364–1368.
11. **Diaz-Guerra, T. M., E. Mellado, M. Cuenca-Estrella, and J. L. Rodriguez-Tudela.** 2003. A point mutation in the 14α-sterol demethylase gene *cyp51A* contributes to itraconazole resistance in *Aspergillus fumigatus*. Antimicrob. Agents Chemother. **47:**1120–1124.
12. **Fedorova, N., et al.** 2008. Genomic islands in the pathogenic filamentous fungus *Aspergillus fumigatus*. PLoS Genet. **4:**e1000046.
13. **Heilmann, C. J., S. Schneider, K. S. Barker, P. D. Rogers, and J. Morschhäuser.** 2010. An A643T mutation in the transcription factor Upc2p causes constitutive *ERG11* upregulation and increased fluconazole resistance in *Candida albicans*. Antimicrob. Agents Chemother. **54:**353–359.
14. **Hey, P., G. Robson, M. Birch, and M. Bromley.** 2008. Characterisation of Aft1 a Fot1/Pogo type transposon of *Aspergillus fumigatus*. Fungal Genet. Biol. **45:**117–126.
15. **Howard, S. J., and M. C. Arendrup.** 2011. Acquired antifungal drug resistance in Aspergillus fumigatus: epidemiology and detection. Med. Mycol. **49**(Suppl. 1):S90–S95.
16. **Howard, S. J., et al.** 2009. Frequency and evolution of azole resistance in *Aspergillus fumigatus* associated with treatment failure. Emerg. Infect. Dis. **15:**1068–1076.
17. **Howard, S. J., et al.** 2006. Multi-azole resistance in *Aspergillus fumigatus*. Int. J. Antimicrob. Agents. **28:**450–453.
18. **Kelly, S. L., D. C. Lamb, A. J. Corran, B. C. Baldwin, and D. E. Kelly.** 1995. Mode of action and resistance to azole antifungals associated with the formation of 14 alpha-methylergosta-8,24(28)-dien-3 beta,6 alpha-diol. Biochem. Biophys. Res. Commun. **207:**910–915.
19. **Lehrnbecher, T., et al.** 2010. Trends in the postmortem epidemiology of invasive fungal infections at a university hospital. J. Infect. **61:**259–265.
20. **Manavathu, E. K., I. Baskaran, S. Krishnan, G. Alangaden, and P. H. Chandrasekar.** 2003. Abstr. 43rd Intersci. Conf. Antimicrob. Agents Chemother., abstr. M-471.
21. **Manavathu, E. K., J. A. Vazquez, and P. H. Chandrasekar.** 1999. Reduced susceptibility in laboratory-selected mutants of *Aspergillus fumigatus* to itraconazole due to decreased intracellular accumulation of the antifungal agent. Int. J. Antimicrob. Agents. **12:**213–219.
22. **Mann, P. A., et al.** 2003. Mutations in *Aspergillus fumigatus* resulting in reduced susceptibility to posaconazole appear to be restricted to a single amino acid in the cytochrome P450 14α-demethylase. Antimicrob. Agents Chemother. **47:**577–581.
23. **Mellado, E., T. M. Diaz-Guerra, M. Cuenca-Estrella, and J. L. Rodriguez-Tudela.** 2001. Identification of two different 14-α sterol demethylase-related genes (*cyp51A* and *cyp51B*) in *Aspergillus fumigatus* and other *Aspergillus* species. J. Clin. Microbiol. **39:**2431–2438.
24. **Mellado, E., et al.** 2007. A new *Aspergillus fumigatus* resistance mechanism conferring in vitro cross-resistance to azole antifungals involves a combination of *cyp51A* alterations. Antimicrob. Agents Chemother. **51:**1897–1904.
25. **Mellado, E., et al.** 2005. Targeted gene disruption of the 14-α sterol demethylase (*cyp51A*) in *Aspergillus fumigatus* and its role in azole drug susceptibility. Antimicrob. Agents Chemother. **49:**2536–2538.
26. **Nam, H. S., et al.** 2010. Clinical characteristics and treatment outcomes of chronic necrotizing pulmonary aspergillosis: a review of 43 cases. Int. J. Infect. Dis. **14:**e479–e482.
27. **Nascimento, A. M., et al.** 2003. Multiple resistance mechanisms among *Aspergillus fumigatus* mutants with high-level resistance to itraconazole. Antimicrob. Agents Chemother. **47:**1719–1726.
28. **Nierman, W., et al.** 2005. Genomic sequence of the pathogenic and allergenic filamentous fungus *Aspergillus fumigatus*. Nature **438:**1151–1156.
29. **Osherov, N., D. P. Kontoyiannis, A. Romans, and G. S. May.** 2001. Resistance to itraconazole in *Aspergillus nidulans* and *Aspergillus fumigatus* is conferred by extra copies of the *A. nidulans* P-450 14alpha-demethylase gene, pdmA. J. Antimicrob. Chemother. **48:**75–81.
30. **Paisley, D., G. D. Robson, and D. W. Denning.** 2005. Correlation between in vitro growth rate and in vivo virulence in *Aspergillus fumigatus*. Med. Mycol. **43:**397–401.
31. **Pfaffl, M. W., G. W. Horgan, and L. Dempfle.** 2002. Relative expression software tool (REST) for group-wise comparison and statistical analysis of relative expression results in real-time PCR. Nucleic Acids Res. **30:**e36.
32. **Pfaller, M. A., et al.** 2009. Wild-type MIC distribution and epidemiological cutoff values for Aspergillus fumigatus and three triazoles as determined by the Clinical and Laboratory Standards Institute broth microdilution methods. J. Clin. Microbiol. **47:**3142–3146.
33. **Pringle, A., et al.** 2005. Cryptic speciation in the cosmopolitan and clonal human pathogenic fungus *Aspergillus fumigatus*. Evolution **59:**1886–1899.
34. **Rodriguez-Tudela, J. L., et al.** 2008. Epidemiological cutoffs and cross-resistance to azole drugs in *Aspergillus fumigatus*. Antimicrob. Agents Chemother. **52:**2468–2472.
35. **Robson, G. D., M. G. Wiebe, B. Cunliffe, and A. P. Trinci.** 1995. Choline- and acetylcholine-induced changes in the morphology of *Fusarium graminearum*:

evidence for the involvement of the choline transport system and acetylcholinesterase. Microbiology **141:**1309–1314.

36. **Slaven, J. W., et al.** 2002. Increased expression of a novel *Aspergillus fumigatus* ABC transporter gene, *atrF*, in the presence of itraconazole in an itraconazole resistant clinical isolate. Fungal Genet. Biol. **36:**199–206.

37. **Snelders, E., et al.** 2008. Emergence of azole resistance in *Aspergillus fumigatus* and spread of a single resistance mechanism. PLoS Med. **5:**e219.

38. **Steele, G. C., and A. P. Trinci.** 1975. Morphology and growth kinetics of hyphae of differentiated and undifferentiated mycelia of Neurospora crassa. J. Gen. Microbiol. **91:**362–368.

39. **Subcommittee on Antifungal Susceptibility Testing (AFST) of the ESCMID European Committee on Antimicrobial Susceptibility Testing EUCAST.** 2008. EUCAST technical note on method for the determination of broth dilution minimum inhibitory concentrations of antifungal agents for conidia-forming moulds. Clin. Microbiol. Infect. **14:**982–984.

40. **Tobin, M. B., R. B. Peery, and P. L. Skatrud.** 1997. An electrophoretic molecular karyotype of a clinical isolate of *Aspergillus fumigatus* and localization of the MDR-like genes *AfuMDR1* and *AfuMDR2*. Diagn. Microbiol. Infect. Dis. **29:**67–71.

41. **Trinci, A. P.** 1974. A study of the kinetics of hyphal extension and branch initiation of fungal mycelia. J. Gen. Microbiol. **81:**225–236.

42. **Verweij, P. E., S. J. Howard, W. J. G. Melchers, and D. W. Denning.** 2009. Azole-resistance in Aspergillus: proposed nomenclature and breakpoints. Drug Resist. Updat. **12:**141–147.

43. **Vogel, H. J.** 1956. A convenient growth medium for *Neurospora* (medium N). Microbiol. Genet. Bull. **13:**42–44.

44. **Walsh, T. J., et al.** 2008. Treatment of aspergillosis: clinical practice guidelines of the Infectious Diseases Society of America. Clin. Infect. Dis. **46:**327–360.